Clear-Sky Bidirectional Reflectance Functions Derived from ARM-UAV MPIR Data Over the ARM Southern Great Plains Site

S. D. Mayor
Analytical Services and Materials, Inc.
Hampton, Virginia

P. Minnis
Atmospheric Sciences Division
NASA-Langley Research Center
Hampton, Virginia

G. S. Phipps
Sandia National Laboratories
Albuquerque, New Mexico

Introduction

Bidirectional reflectance distribution functions (BRDFs) quantify the anisotropic reflection of radiation. At the top of the atmosphere, the surface and the atmosphere affect the anisotropy of the reflected solar radiation. BRDFs are essential for deriving albedos from radiances measured by satellites and for predicting the radiance field for a given set of conditions. Measurements of complete BRDFs are difficult to obtain at the top of the atmosphere (TOA). Usually radiances are collected by a satellite from different angles over particular scene types for many orbits to obtain sufficient data for BRDF development. The data are compromised in angular coverage and scene consistency. Aircraft missions are too limited temporally to cover a sufficient range of solar zenith angles (SZAs) to complete the BRDFs. Unmanned aerospace vehicles (UAV), however, can remain aloft over the same area for relatively long time periods. Data taken by the high-resolution multispectral pushbroom imaging radiometer (MPIR) on the Atmospheric Radiation Measurement (ARM)-UAV during the Fall 1996 Flight Series are used to derive a set of visible channel clear-sky BRDFs for the ARM Southern Great Plains (SGP) site to improve the cloud and albedo products derived from the Geostationary Operational Environmental Satellite (GOES).

Data

The MPIR was built and fielded by Sandia National Laboratories in Albuquerque, New Mexico, to provide quantitative radiance data in nine spectral bands. The instrument was mounted downlooking on the UAV during the Fall 96 Intensive Observation Period (IOP) with an 11° tilt to port. The cross-track field-of-view is ±40°. The surface resolution is ~0.1 km at a UAV altitude of 15 km. Only high resolution channel-1 (645 nm) data from 3 days (September 29, October 3, and October 5, 1996) were used in this study to derive visible channel clear-sky BRDFs. Data from these flights were taken at altitudes between 6 km and 12 km at viewing zenith angles (VZAs) between 0° and 60° because of the limited cant of the MPIR on the UAV. Most flights occurred near noon (SZA ~45°), but data from one 24-hour flight covered higher SZAs (53° to 90°).

Methodology

To describe the angular variation of radiance, the angular coordinates were divided into ranges called "bins," and the model was represented by mean values for each bin. These bins were defined by increments of 10° VZA, 15° relative azimuth angle (except the first two and last two bins were 7.5°), and 10° SZA. Data from all 3 days were averaged into these bins.

Because the albedo of land surfaces, especially bare soil, varies as a function of surface dampness, the 3 days were evaluated for wet/dry conditions. A plot of the diurnal variation of albedo in the 0.5° box around the SGP Cloud and Radiation Testbed (CART) site from GOES-8 (Figure 1) showed a significantly lower albedo for September 29 compared to October 3, indicating the ground was still wet from rains that occurred on September 26.

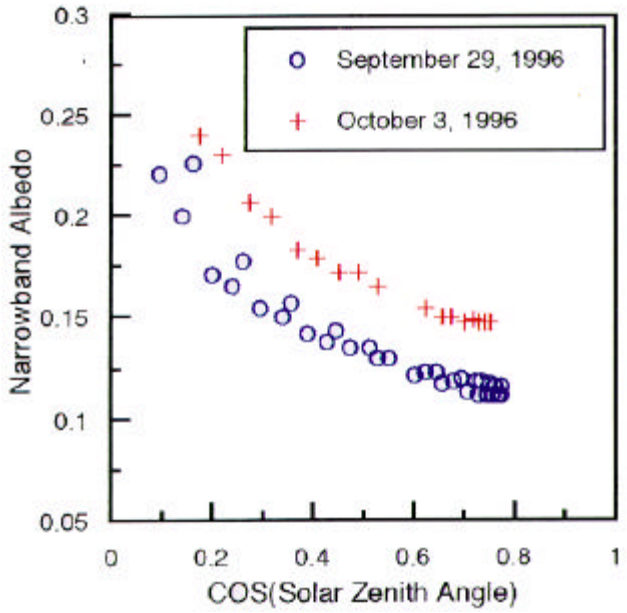

Figure 1. Clear-sky narrowband visible albedos derived from GOES-8 for a 0.5° box centered at the central facility. (For a color version of this figure, please see *http://www.arm.gov/docs/documents/technical/conf_9803/mayor-98.pdf*.)

Thus, MPIR reflectances from September 29 were normalized to the October 3 albedo from GOES.

To apply the model to satellite data, the reflectances from MPIR were corrected to the top of the atmosphere by accounting for molecular scattering and ozone absorption. For this analysis, all aerosols were assumed to be below the UAV. The correction for ozone absorption and Rayleigh scattering follow the procedures of Minnis et al. (1993). The reflectance parameterization is described below.

The reflectance at the TOA is

$$\rho_{TOA} = t_u \left[\rho_{ray}(\mu_o, \mu, \psi) + \rho_{mpir}(\mu_o, \mu, \psi)\right] \qquad (1)$$

where t_μ is the upward transmittance and ρ_{ray} is the reflectance of overlying Rayleigh layer. The reflectance at the MPIR, ρ_{mpir}, is defined as

$$\rho_{mpir} = \frac{R_{meas}}{E_\lambda (1-\alpha_{ray}) t_{a1}} \qquad (2)$$

where

α_{ray} = the albedo of Rayleigh layer above the UAV
E_λ = the spectral solar constant (value used in this analysis for MPIR channel 1 is 73.88 Wm^{-2})
R_{meas} = the radiance measurement at flight level
t_{a1} = the transmittance of ozone above the UAV
μ = cos(SZA)
μ_o = cos(VZA)
ψ = the relative azimuth angle.

For this analysis, the ozone absorption optical depth for the visible channel is fixed at 0.027, a value that corresponds to an ozone path length of 0.35 cm-STP.

The corrected radiances in the angular bins were then combined using pixel-weighted averages over the 3 days.

$$\sum_{sz,vz,az} \frac{\sum_{day=1}^{3} n_{day}\ \mu_{o_{day}}\ L_{day}}{\sum_{day=1}^{3} n_{day}\ \mu_{o_{day}}}$$

where n = number of pixels in the bin and L = radiance.

Due to the limited cross-track field-of-view (FOV) of the MPIR on the UAV and limited hours of flight data, not all VZA and SZA bins were filled. The most serious problem was values missing for entire SZA bins. To fill some of the empty bins, the Helmholtz Principle of Reciprocity,

$$\mu_o L(\mu_o, \psi; \mu) = \mu L(\mu, \psi; \mu_o)$$

was applied first. For reciprocal bins with data, the difference between the observed and predicted radiances (Figure 2) is unbiased with a root-mean-square difference of 15.8% indicating that the use of this principle here is justified. Much of the scatter is probably due to the variations in the observed scenes.

To complete the model, the radiances missing at low VZA bins for low SZAs were predicted from radiances in bins with data and corrected with the narrowband BRDFs of Minnis and Harrison (1984; MH). Similarly, Earth Radiation Budget Experiment (ERBE) BRDFs (Suttles et al. 1988) were used with the filled bins to fill empty high VZA bins at high SZAs.

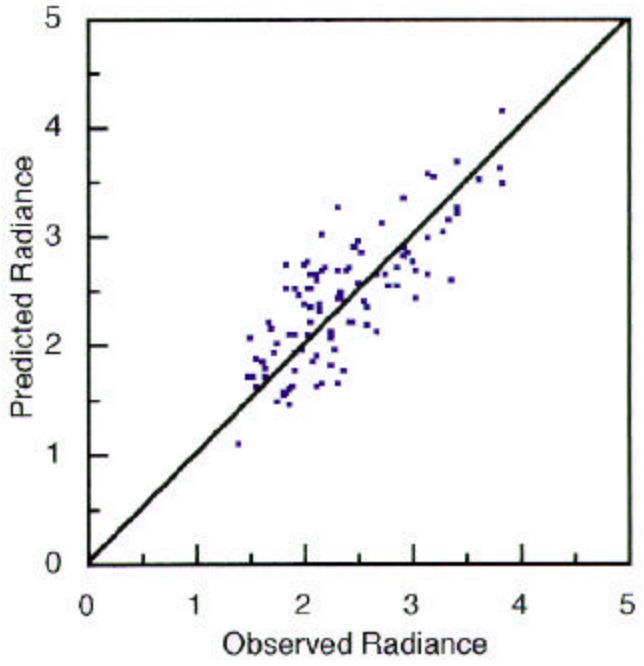

Figure 2. Application of reciprocity to filled angular bins yielded an root mean square (rms) of 15.8% with bias = -0.0054 (radiance is in $Wm^{-2}sr^{-1}$). (For a color version of this figure, please see *http://www.arm.gov/docs/documents/technical/conf_9803/mayor-98.pdf*.)

Results

The MPIR data were used to generate reflectances at the instrument altitude and at the TOA. Figure 3a shows the combined MPIR-measured reflectances from all 3 days at flight level for an SZA of 45°. Though MPIR can only observe up to ±40° VZA, the 11° tilt to port reduces the VZA to 29° in one direction and increases it to 51° in the other. Furthermore, banks in the UAV increased the VZA to almost 60°.

Next, the MPIR reflectances were computed at the TOA by applying equations (1) and (2). These corrections increased the reflectances by about 20% overall as shown in Figure 3b. Finally, the TOA reflectances were integrated over all angles and normalized to create the BRDF models. The MPIR-derived BRDF for SZA = 45° is shown in Figure 3c. For this example, only reciprocity was necessary to fill missing bins. For higher SZAs, reciprocity and ERBE BRDFs were applied to fill missing high VZA bins. For models at lower SZA, reciprocity and MH BRDFs filled the missing low VZA bins.

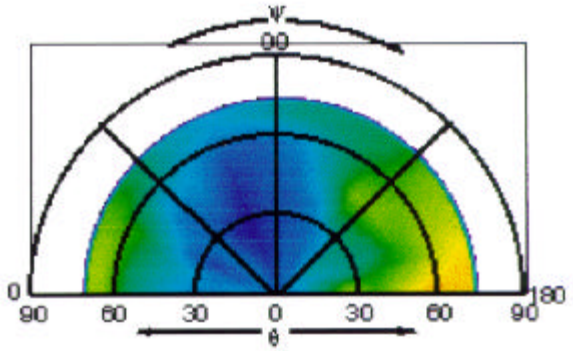

Figure 3a. MPIR-measured reflectances averaged over 3 days at flight altitude (SZA = 45°).

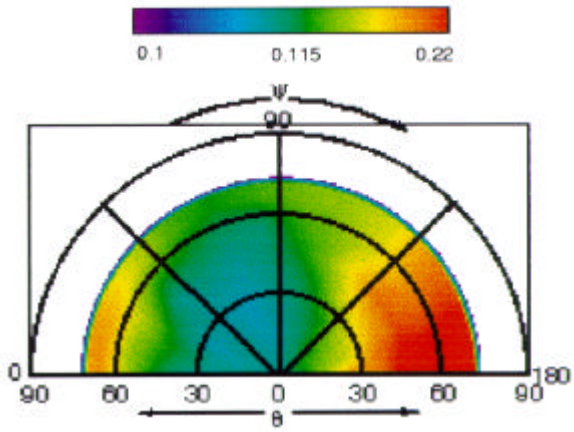

Figure 3b. MPIR-measured reflectances averaged over 3 days and corrected to TOA (SZA = 45°).

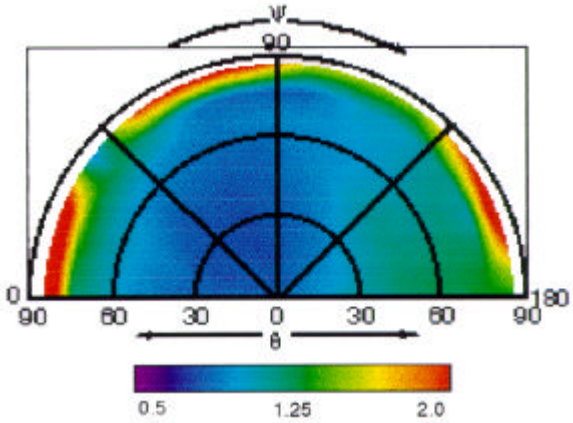

Figure 3c. Anisotropic visible reflectance factors derived from ARM/UAV MPIR measurements over SGP (SZA = 45°).

(For a color version of Figure 3, please see *http://www.arm.gov/docs/documents/technical/conf_9803/ mayor-98.pdf*.)

In general, the anisotropic factors have small variations over the first three SZA bins (not shown), but significant increases in the forward and back scattering peaks are observed at higher SZAs. Figures 4 and 5 compare the MPIR-derived and MH BRDFs for SZA = 55° and 75°, respectively. The major features of the two models are similar. Overall, the MPIR BRDFs show more structure than the MH models. The MH models are most likely smoother because they are derived from low-level aircraft data taken over a wide variety of land regions while the MPIR data were limited to the ARM SGP region and contain estimates for some bins. The MH models were not corrected to the TOA. Both models become more anisotropic with increasing SZA. The models also show a strong backscattering peak near the anti-solar point and a minimum near nadir in the forward scattering direction.

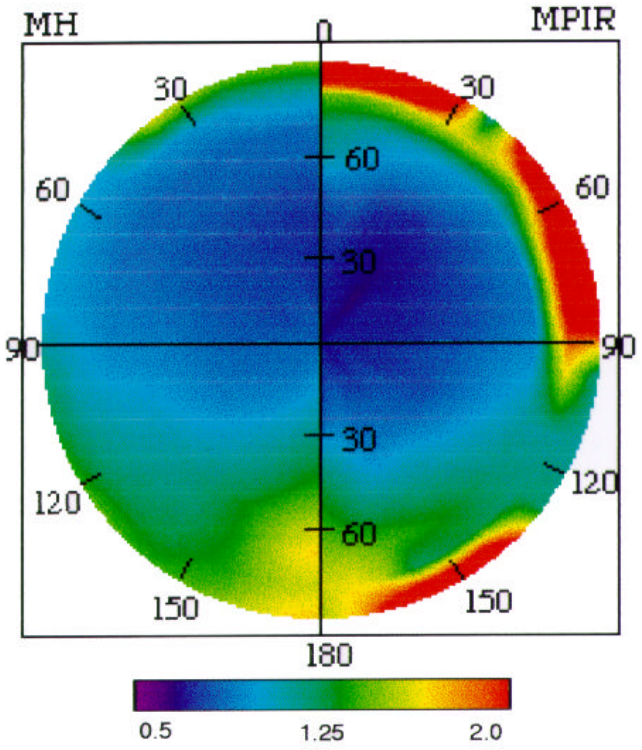

Figure 4. Comparison of anisotropic visible reflectance factors derived from ARM/UAV MPIR measurements over SGP and MH BRDF (SZA=55°). (For a color version of this figure, please see *http://www.arm.gov/docs/documents/technical/conf_9803/mayor-98.pdf*.)

The MPIR model will be tested using simultaneous visible channel observations from multiple GOES and Sun-synchronous satellites. Reflectance from a scene observed by one satellite is used with the BRDF model to predict the reflectance for the other satellite. This approach to estimating the model errors is currently under way.

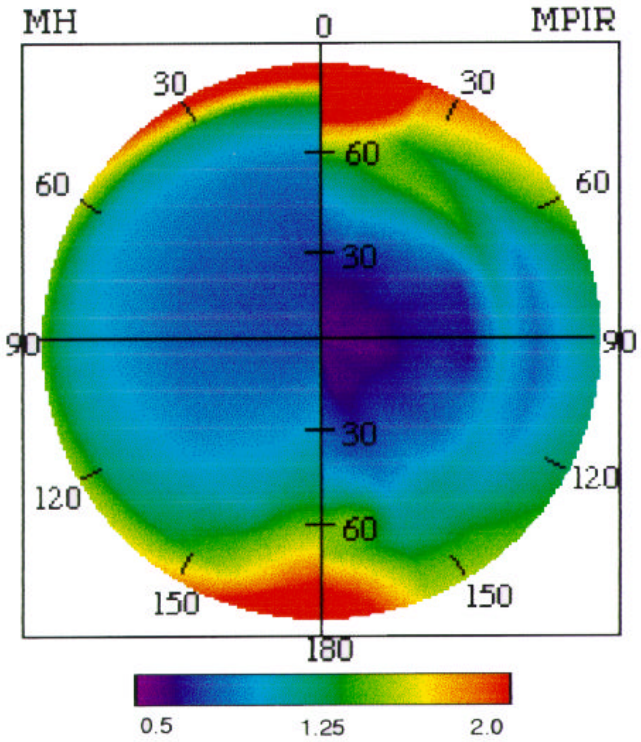

Figure 5. Comparison of anisotropic visible reflectance factors derived from ARM/UAV MPIR measurements over SGP and MH BRDF (SZA=75°). (For a color version of this figure, please see *http://www.arm.gov/docs/documents/technical/conf_9803/mayor-98.pdf*.)

Conclusions

The MPIR-based BRDF model should improve accuracy of ARM satellite-derived cloud and radiation products because it is specifically representative of the SGP area. Despite its limited coverage, the major features of the model compared reasonably well with the MH and ERBE BRDFs. Because of its high ceiling, the UAV/MPIR can provide BRDFs useful for satellite interpretation without relying on models to account for aerosol and atmospheric scattering. Filling missing angular bins increased uncertainty in the derived BRDF model. Hence, data from additional clear-sky UAV flights are needed to fill more bins and reduce dependence on auxiliary bin filling techniques. While the UAV/MPIR provides unprecedented SZA coverage for a given surface, future flights would be even more useful if the MPIR tilt were increased to 40° to enable measurement of radiances

over almost all VZAs. That configuration would nearly eliminate the potentially large uncertainties due to bin filling.

Acknowledgments

This research was conducted under U.S. Department of Energy Interagency Agreement DE-AI05-95ER61992 as part of the ARM/UAV Program. Sean Moore of Mission Research Corporation, Santa Barbara, California provided assistance in the development of software to geolocate the MPIR radiances.

References

Minnis, P., and E. F. Harrison, 1984: Diurnal variability of regional cloud and clear-sky radiative parameters derived from GOES data; Part 1: analysis method. *J. Climate Appl. Meteorol*., **23**, 993-1011.

Minnis, P., K. Liou, and Y. Takano, 1993: Inference of cirrus cloud properties using satellite-observed visible and infrared radiances. I - Parameterization of radiance fields. *J. Atmos. Sci*., **50**, 1279-1304.

Suttles, J. T., R. N. Green, P. Minnis, G. L. Smith, W. F. Staylor, B. A. Wielicki, I. J. Walker, D. F. Young, V. R. Taylor, and L. L. Stowe, 1988: Angular radiation models for earth-atmosphere system, vol. 1. *Shortwave Radiation*, NASA Ref. Publ., 1184.